

Inhibition of Endothelial Cell Proliferation and Tumor Angiogenesis by Up-Regulating *NDRG2* Expression in Breast Cancer Cells

Ji Ma^{1,2,3,9}, Wenchao Liu^{1*9}, Xiaohong Yan^{4,9}, Qianrong Wang^{1,9}, Qingli Zhao³, Yan Xue¹, Hui Ren³, Lin Wu², Yuanxiong Cheng⁵, Sen Li¹, Lu Miao⁶, Libo Yao², Jian Zhang^{2*}

1 Department of Oncology, Xijing Hospital, The State Key Discipline of Cell Biology, The Fourth Military Medical University, Xi'an, Shaanxi Province, China, **2** The State Key Laboratory of Cancer Biology, Department of Biochemistry and Molecular Biology, The Fourth Military Medical University, Xi'an, Shaanxi Province, China, **3** Department of Breast Surgery, Lanzhou General Hospital of CPLA, Lanzhou, Gansu Province, China, **4** Department of Oncology, Baoji Central Hospital, Baoji, Shaanxi Province, China, **5** Department of Respiratory, Nanfang Hospital, Southern Medical University, Guangzhou, Guangdong Province, China, **6** School of Aerospace Medicine, The Fourth Military Medical University, Xi'an, Shaanxi Province, China

Abstract

The N-myc downstream-regulated gene 2 (*NDRG2*) is involved in tumor cell differentiation and apoptosis, but its function in tumor angiogenesis remains to be established. Here, we employed adenovirus overexpressing *NDRG2* (Ad-*NDRG2*) to efficiently up-regulate target gene expression in the *NDRG2*-low-expressing, breast cancer cell line MCF-7. Moreover, VEGF secretion was decreased in MCF-7 cells infected by Ad-*NDRG2*, and medium conditioned by these infected cells could significantly inhibit the proliferation, tube formation and invasion of human umbilical vein endothelial cells (HUVECs). Further study indicated that the angiogenesis promoting factors VEGF and HIF-1 α were down-regulated, whereas the angiogenesis suppressing factors p53 and VHL were up-regulated in MCF-7 cells infected by Ad-*NDRG2*. Finally, in a nude mouse model, intratumoral injections of Ad-*NDRG2* every 3 days for 20 days significantly inhibited the growth and angiogenesis of xenografted MCF-7 tumors. In summary, these data indicate that *NDRG2* may be involved in angiogenesis by impacting the expression of angiogenesis related factors. Thus, specific overexpression of *NDRG2* by adenovirus represents a promising approach for the treatment of tumor angiogenesis.

Citation: Ma J, Liu W, Yan X, Wang Q, Zhao Q, et al. (2012) Inhibition of Endothelial Cell Proliferation and Tumor Angiogenesis by Up-Regulating *NDRG2* Expression in Breast Cancer Cells. PLoS ONE 7(2): e32368. doi:10.1371/journal.pone.0032368

Editor: Ming Tan, University of South Alabama, United States of America

Received: October 20, 2011; **Accepted:** January 26, 2012; **Published:** February 29, 2012

Copyright: © 2012 Ma et al. This is an open-access article distributed under the terms of the Creative Commons Attribution License, which permits unrestricted use, distribution, and reproduction in any medium, provided the original author and source are credited.

Funding: This work was supported by grants from the National Nature Science Foundation of China (nos. 30830054, 81172292, 81071894, 81072050 and 30572100) and Nation Program on Key Basic Research Project (2009CB521704). The funders had no role in study design, data collection and analysis, decision to publish, or preparation of the manuscript.

Competing Interests: The authors have declared that no competing interests exist.

* E-mail: biozhangj@yahoo.com.cn (JZ); xjcancer@fmmu.edu.cn (WL)

⁹ These authors contributed equally to this work.

Introduction

Breast cancer neovascularization (BCN), involving both angiogenesis and vasculogenesis, is a key event in tumorigenesis, invasion and metastasis. In recent decades, significant progress has been made toward understanding the pathophysiologic mechanisms of BCN. However, the development of BCN is a complicated and dynamic process, involving multiple stimuli, multiple cytokines and multiple cell-type participation, and the specific mechanisms underlying its progression are largely unknown.

Hypoxia, a common feature of malignant tumors, can be detected in central regions of solid tumors as well as during embryonic development [1]. Hypoxia regulates many transcription factors, including hypoxia-inducible factor (HIF)-1 α , which controls hypoxia-induced angiogenic factors such as vascular endothelial growth factor (VEGF) [2]. VEGF functions as a survival factor in endothelial cells and tumor cells via VEGF receptors that are also up-regulated by hypoxia [3]. Thus, increased VEGF expression by hypoxia, and thereby promotion

of angiogenesis, may be a prerequisite for progressive growth and metastasis of solid tumors, such as breast cancer. The tumor suppressor genes p53 and VHL inhibit angiogenesis [4,5]. Mutation or loss of function of these suppressors results in high vascularization in malignant tumors. VHL and p53 could promote degradation of HIF-1 α by ubiquitin-mediated proteolysis and suppress HIF-1 α -stimulated transcription [6]. VEGF expression is negatively regulated by p53 and VHL and is frequently overexpressed along with HIF-1 α in human cancers [4,7]. To understand the interactions between angiogenesis promoting factors and angiogenesis suppressing factors, it is necessary to develop treatment strategies that specially target BCN.

NDRG2, a member of the N-myc downstream-regulated gene family, belongs to the alpha/beta hydrolase superfamily. It was first cloned in our laboratory from a normal human brain cDNA library by subtractive hybridization (GenBank accession no. AF159092) and is regarded as a tumor suppressor gene (TSG) that is transcriptionally repressed by c-Myc [8,9,10]. Accumulated evidence indicates that *NDRG2* is down-regulated or undetectable in many human cancers [11,12]. The role of

NDRG2 in breast cancer has also been studied. Recently, it has been shown that breast cancer cells have low or undetectable expression of *NDRG2* compared with the high expression of *NDRG2* in normal tissues [13]. Further studies have found that *NDRG2* is able to inhibit proliferation and enhance apoptosis in many malignant tumors [14]. In addition, *NDRG2* could induce BMP-4 expression and inhibit the metastatic potential of breast cancer cells, specifically via suppression of MMP-9 activity [15]. In our previous study, we have verified also that, as a regulator, *NDRG2* could modulate the process of breast cancer cell adhesion and invasion through regulating CD24 expression [16]. However, the specific effect of *NDRG2* on breast cancer angiogenesis is still unknown.

In this study, we first demonstrate that *NDRG2* is a regulator participating in the progression of breast cancer angiogenesis. Using adenovirus *NDRG2* expression, we verified that Ad-*NDRG2* could decrease VEGF secretion by MCF-7 cells, and this MCF-7 conditioned medium significantly inhibited HUVEC proliferation, tube formation and invasion. Furthermore, Ad-*NDRG2* up-regulated the expressions of p53 and VHL while down-regulating the expressions of VEGF and HIF-1 α . Ad-*NDRG2* also inhibited tumor growth and angiogenesis in a nude mouse model. Our results present a novel role for *NDRG2* in the regulation of breast cancer angiogenesis.

Results

NDRG2 expression in breast cancer cell lines

The tumor suppressor gene *NDRG2* is down-regulated or undetectable in many human cancers. Here, *NDRG2* expression in seven breast cancer cell lines was investigated by western blot and RT-PCR. The results showed that the expression of *NDRG2* was higher in ZR-751 and T47D cell lines and lower in MDA-MB-231 and MCF-7 cell lines (Fig. 1A). To further determine the role of *NDRG2*, we chose to use MCF-7 cells (with wild-type p53) as our experimental model in the following studies.

NDRG2 up-regulation by Ad-*NDRG2* in MCF-7 cells

To evaluate the up-regulation of *NDRG2* expression, western blot and RT-PCR analyses were performed. As shown in Figure 1B, after infection by Ad-*NDRG2*, the expression of *NDRG2* was successfully increased at both the protein and mRNA levels in MCF-7 cells, which express a low level of endogenous *NDRG2*.

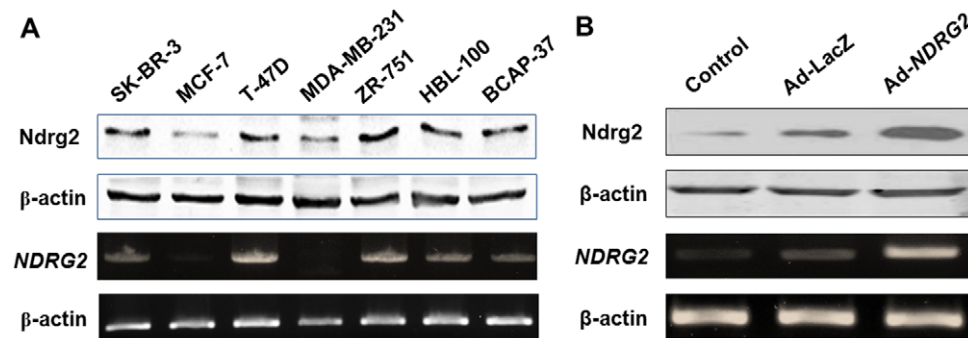


Figure 1. Expression of *NDRG2* in breast cancer cell lines and the effect of Ad-*NDRG2*. (A) T-47D, MCF-7, BCAP-37, HBL-100, ZR-751, SK-BR-3 and MDA-MB-231 cells were collected for extraction of protein and RNA and analyzed for *NDRG2* expression using western blot and RT-PCR. (B) *NDRG2* low-expression MCF-7 breast cancer cells were infected by adenovirus carrying *NDRG2* (Ad-*NDRG2*) or negative control LacZ (Ad-LacZ). Thereafter, protein and RNA from these cells were extracted and subjected to western blot and RT-PCR analysis. β -actin was used as a loading control. The data are representative of three independent experiments. doi:10.1371/journal.pone.0032368.g001

Suppression of HUVEC proliferation by up-regulating *NDRG2* in MCF-7 cells

To investigate the effect of *NDRG2* up-regulation in MCF-7 cells on HUVEC proliferation, an MTT assay was designed. First, HUVECs grown in serum-free medium conditioned by MCF-7 cells showed an increase in the proliferation rate, as revealed by the culture time (Fig. 2A). Next, medium conditioned by Ad-*NDRG2* infected MCF-7 cells markedly inhibited HUVEC proliferation, which correlated with the conditioning time of the medium (Fig. 2B). Notably, compared to normoxic conditions, these effects were much more significant under hypoxic conditions.

Alterations of HUVEC tube formation and invasion by regulating *NDRG2* in MCF-7 cells

To test the effect of *NDRG2* on angiogenesis, tube formation and invasion assays of HUVECs were performed on Matrigel under hypoxia. Ad-*NDRG2* and *NDRG2* siRNA (si-*NDRG2*) were applied respectively to overexpress or knockdown *NDRG2*. As the control group, Ad-LacZ-MCF-7 or scramble-MCF-7 cells, HUVECs associated with one another and formed microtubes after 6 h. The medium from Ad-*NDRG2*-MCF-7 cells could repress the tube formation of HUVECs, but that from si-*NDRG2*-MCF-7 cells promoted the tube formation of HUVECs (Fig. 3A and 3B). The invasion assay revealed that the medium from Ad-*NDRG2*-MCF-7 cells inhibited HUVECs' invasion ability; however, that from si-*NDRG2*-MCF-7 cells increased a lot compared with the Ad-LacZ-MCF-7 or scramble-MCF-7 cells respectively (Fig. 3C and 3D). These data raised the possibility that *NDRG2* overexpression or knockdown in MCF-7 cells might mediate the production of extracellular matrix components that in turn are involved in the tube formation and invasion of HUVECs.

Regulation of the expression of hypoxia-induced, angiogenesis related factors by up-regulation of *NDRG2* in MCF-7 cells

To further explore whether products of resulting from *NDRG2* up-regulation in MCF-7 cells may be responsible for inhibition of HUVEC growth, we measured the VEGF level in cell culture medium under normoxic or hypoxic conditions. ELISA assay results showed that, compared to normoxic conditions, hypoxia could significantly increase VEGF secretion into the cell culture medium in a time-dependent manner (Fig. 4A). Furthermore, VEGF secretion was decreased in MCF-7 cells infected by Ad-

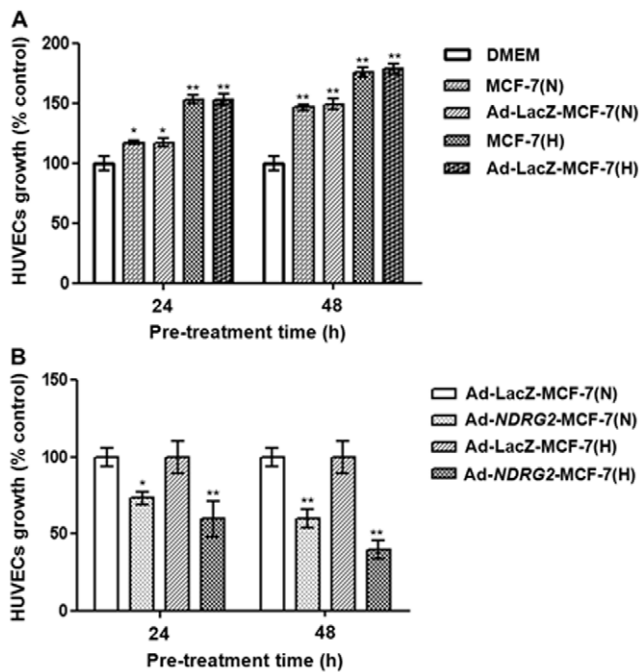


Figure 2. Effect of MCF-7 preconditioned media on HUVEC proliferation. (A) HUVECs were grown to confluence and were then cultured in preconditioned media (derived from MCF-7 and Ad-LacZ-MCF-7 cells pretreated under normoxia and hypoxia for 24 or 48 h) for 24 h, and serum-free DMEM was used as a control. (B) HUVECs were grown to confluence and were then cultured in preconditioned media (derived from Ad-LacZ-MCF-7 or Ad-*NDRG2*-MCF-7 cells pretreated under normoxia and hypoxia for 24 or 48 h) for 24 h. Ad-LacZ-MCF-7(N) or Ad-LacZ-MCF-7(H) was used as controls. N, normoxia; H, hypoxia. The data are the mean \pm standard deviation (SD) for three independent experiments. Statistical significance was assessed using one-way ANOVA and Student's *t*-test. * or ** indicates $P < 0.05$ or $P < 0.01$, respectively, when compared with the control. doi:10.1371/journal.pone.0032368.g002

NDRG2 in a time-dependent manner, especially under hypoxic conditions (Fig. 4B). To determine whether these hypoxia-induced, angiogenesis related factors are involved in *NDRG2*-mediated cell activities in breast cancer, western blot was performed to examine the expression levels of these factors. The results showed that HIF-1 α expression was decreased in Ad-*NDRG2*-MCF-7 cells, and this was in accordance with the decreased VEGF secretion. In contrast to the effect on VEGF and HIF-1 α , the expressions of p53 and VHL were up-regulated by Ad-*NDRG2* under hypoxia (Fig. 4C). Thus, it is possible that *NDRG2* influences HIF-1 α and VEGF expression by indirectly regulating p53 and VHL expression or by directly controlling the transcription of HIF-1 α and VEGF.

Suppression of tumor growth and angiogenesis in a nude mouse model by intratumoral injection of Ad-*NDRG2*

To investigate the effects of Ad-*NDRG2* on tumor growth and angiogenesis *in vivo*, we injected 1×10^9 PFU Ad-*NDRG2*, Ad-LacZ or PBS every 3 days into pre-established, human MCF-7 breast tumors (approximately 200 mm³) grown in nude mice. As shown in Figure 5A, the Ad-*NDRG2* group achieved a sustained and significant arrest of tumor growth (71% decrease in mean tumor volume on day 21 compared with the control group), whereas the growth of tumors injected with Ad-LacZ was not significantly

inhibited (3.4% decrease compared with the control group). The mice were sacrificed at 21 days after beginning intratumoral injections, and the tumors were removed for analysis of the vascularization. Immunolabeling for VEGF and HIF-1 α were lower in tumors excised from mice in the Ad-*NDRG2* group. Moreover, the p53 and VHL expression levels in the Ad-*NDRG2* group were dramatically increased dramatically compared to the control group. The microvessel density (MVD) of the tumors was examined after immunolabeling for CD31, a typical vascular endothelial cell marker. In the Ad-*NDRG2* group, the MVD of the tumors was inhibited compared with the control and Ad-LacZ groups. There was no significant difference between the control and Ad-LacZ groups (Fig. 5B and 5C).

Discussion

Although surgical resection, adjuvant and endocrine therapy are commonly used to treat breast cancer patients, the overall survival rate for breast cancer requires improvement. Therefore, the development of biological therapies for breast cancer is urgently required. Recent reports have shown, in breast cancer patients, that *NDRG2* expression is significantly reduced compared to breast normal tissue [13]. Further studies have found that *NDRG2* inhibits the proliferation, adhesion and invasion of breast cancer cells [14,16]. In addition, our previous study found that *NDRG2* could inhibit the metastatic potential of breast cancer cells, specifically via suppression of CD24 or MMP-9 expression [16]. Interestingly, silencing *NDRG2* attenuates p53-mediated apoptosis, whereas overexpression of *NDRG2* suppresses tumor cell growth regardless of the presence or absence of p53 [14]. Therefore, *NDRG2* is required for p53-mediated apoptosis but not for proliferation. These data indicate that an association exists between *NDRG2* expression and reduced breast cancer malignant behavior and that *NDRG2* may be a novel target for future biological therapies for breast cancer. However, to date, the roles of *NDRG2* in breast cancer angiogenesis have not been explored. In this paper, our data revealed that *NDRG2* overexpression in breast cancer cells could suppress HUVEC proliferation, tube formation and invasion by reducing VEGF and HIF-1 α expression and increasing p53 and VHL expression. Importantly, tumor growth and angiogenesis in a nude mouse model were inhibited by intratumoral injection of Ad-*NDRG2*.

Recently, several reports have shown that *NDRG2* is a target gene of HIF-1 α , and hypoxia treatment dramatically up-regulated *NDRG2* expression in many human cancer cell lines [17,18]. Knockdown of HIF-1 α expression did not change *NDRG2* expression but could abolish hypoxia-induced up-regulation of *NDRG2*. In our study, infection by Ad-*NDRG2* reduced HIF-1 α expression in a time-dependent manner in MCF-7 cells. Based on these results, we believe that *NDRG2* is a hypoxia-regulated gene, *NDRG2* and HIF-1 α could regulate each other, and there might be feedback loops between them. Furthermore, our data showed that VEGF secretion was decreased in MCF-7 cells infected by Ad-*NDRG2* in a time-dependent manner, especially under hypoxic conditions. This suggests that *NDRG2* may be involved in hypoxia-induced angiogenesis.

Loss of wild type p53 and VHL could promote angiogenesis by relieving inhibition of VEGF production. Several findings demonstrated that p53 and VHL could inhibit VEGF expression by regulating the transcriptional activity of Sp1 and by down-regulating Src kinase activity under hypoxia [19,20]. Moreover, both p53 and VHL can promote the degradation of HIF-1 α to indirectly suppress VEGF expression [21,22,23]. There is evidence

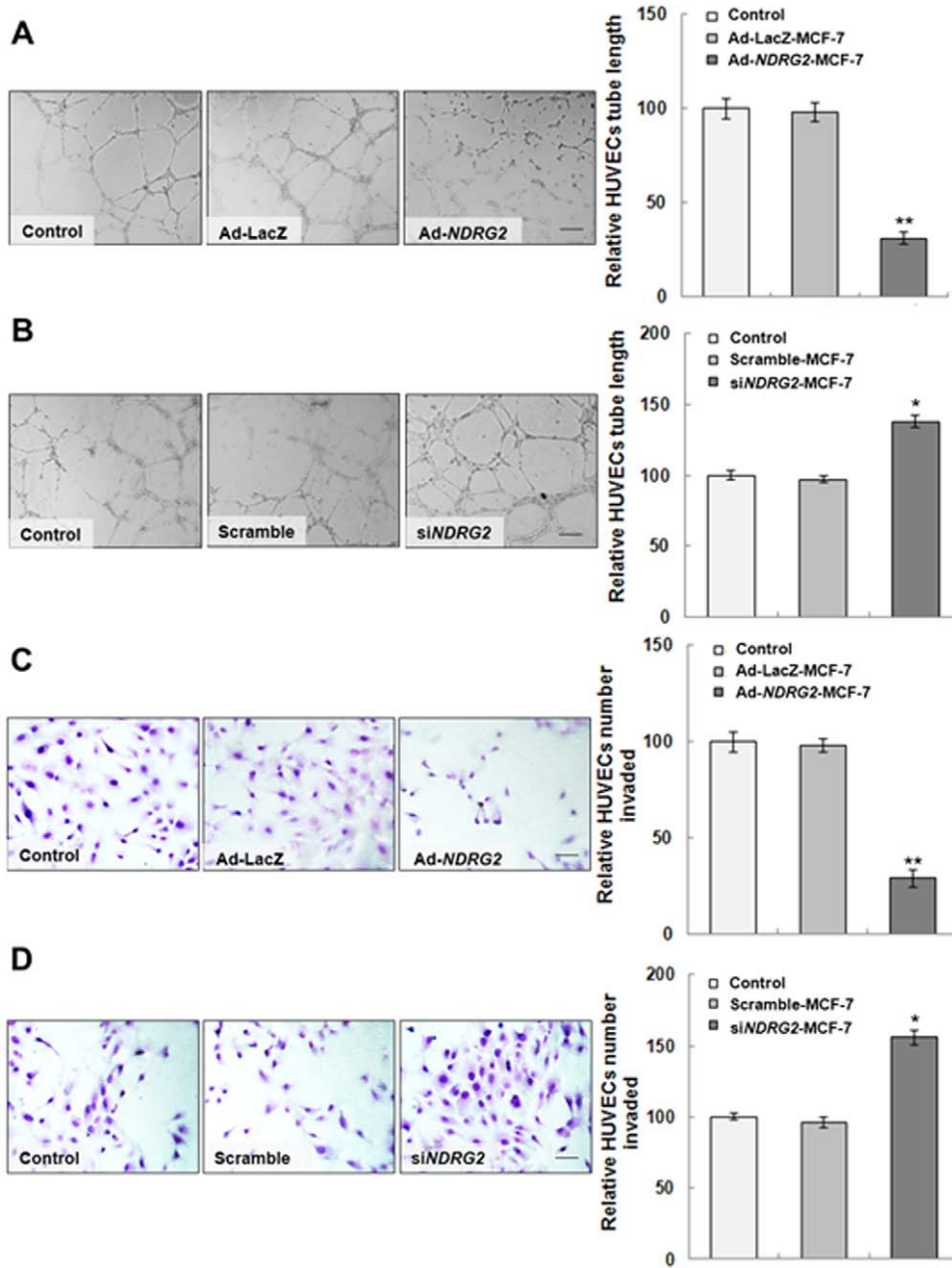


Figure 3. Effect of MCF-7 preconditioned media on HUVEC tube formation and invasion. (A and B) The tube formation assay was performed as described in Material and Methods. HUVECs were plated on Matrigel and incubated under hypoxia for 6 h. Tube lengths were measured with Image-Pro Plus software; the histograms represent the quantification of the tube length of HUVECs. (C and D) The invasion assay was performed as described in Material and Methods. After 4 h under hypoxia, the amount of invaded cells was calculated in five random high-power fields (400 \times), and the number from the control group was used as a control. The histogram represents the quantification of cells that invaded. The data are the mean \pm standard deviation (SD) for three independent experiments. Statistical significance was assessed using one-way ANOVA and Student's *t*-test. * or ** indicates $P < 0.05$ or $P < 0.01$, respectively, when compared with the control. doi:10.1371/journal.pone.0032368.g003

indicating that the expression of VEGF is negatively regulated by p53 and VHL and is frequently overexpressed along with HIF-1 α in human cancers.

The present study has shown that *NDRG2* overexpression in breast cancer cells can inhibit the proliferation, tube formation and invasion of HUVECs, preventing the participation of these cells in hypoxia-induced, tumor angiogenesis. This effect may be related to the inhibition of VEGF secretion. Both *in vitro* and *in vivo* up-regulation of *NDRG2* by Ad-*NDRG2* increased p53 and VHL

expression and decreased VEGF expression. It is possible that the down-regulation of VEGF by *NDRG2* overexpression might be the consequence of the up-regulation of the tumor suppressor genes p53 and VHL. In summary, our results provide the first evidence that *NDRG2* contributes to breast cancer angiogenesis by controlling the expression of angiogenesis related factors. Further investigation into the molecular mechanism of *NDRG2* action may offer a novel approach for treating breast cancer, specifically by targeting breast cancer angiogenesis.

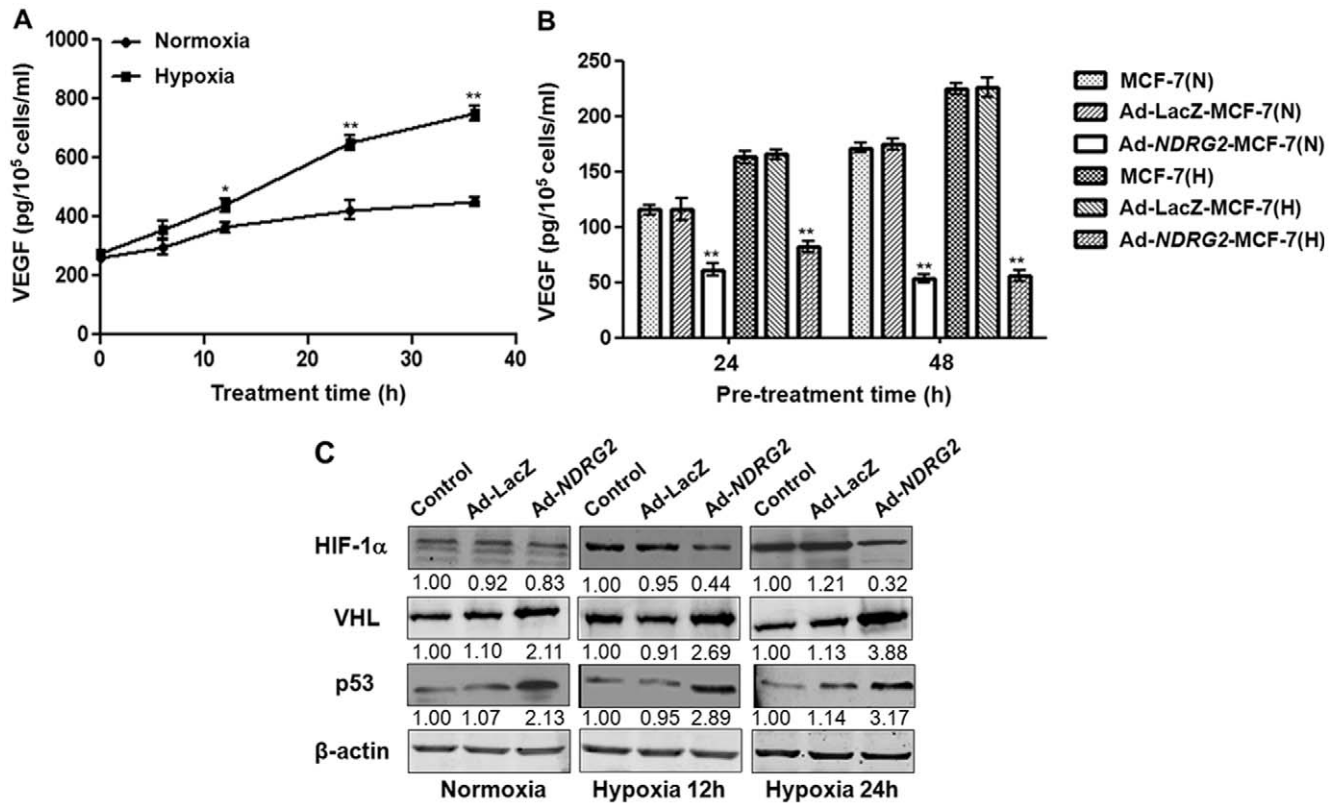


Figure 4. Effect of Ad-NDRG2 on the expression of VEGF, HIF-1 α , p53, and VHL under normoxia or hypoxia. (A) MCF-7 cells were incubated for the indicated time (0, 6, 12, 24, 36 h) in normoxic (21% O₂) or hypoxic (1% O₂) conditions. After incubation, the media were analyzed for VEGF levels by ELISA assay, and the cell number was counted. (B) MCF-7, Ad-LacZ-MCF-7 and Ad-NDRG2-MCF-7 cells were incubated for the indicated time (24, 48 h) in normoxic or hypoxic conditions. After incubation, the media were analyzed for VEGF levels by ELISA assay, and the cell number was counted. The data are the mean \pm standard deviation (SD) for three independent experiments. Statistical significance was assessed with one-way ANOVA and Student's *t*-test. * or ** indicates $P < 0.05$ or $P < 0.01$, respectively, when compared with the normoxia or Ad-LacZ-MCF-7 group. N, normoxia; H, hypoxia. (C) MCF-7, Ad-LacZ-MCF-7 and Ad-NDRG2-MCF-7 cells were incubated under hypoxia for 0, 12, or 24 h. After incubation, the cells were analyzed by western blot assay. β -actin protein levels were used as a loading control. doi:10.1371/journal.pone.0032368.g004

Materials and Methods

Cell lines and reagents

Human breast cancer cell lines T-47D, MCF-7, BCAP-37, HBL-100, ZR-751, SK-BR-3 and MDA-MB-231, were obtained from the American Type Culture Collection (ATCC, USA) and cultured according to their directions and guidelines. Human umbilical vein endothelial cells (HUVECs) were obtained and cultured as described previously [21,22]. HUVECs were suspended in HuMedia-EG2 medium (Kurabo Industries) and then plated on plastic culture dishes. HuMedia-EG2 medium consisted of the base medium (HuMedia-EB2) supplemented with 2% fetal bovine serum, 10 ng/ml hEGF, 5 ng/ml hFGF-B, 1 μ g/ml hydrocortisone, 50 μ g/ml gentamicin, 50 ng/ml amphotericin B, and 10 μ g/ml heparin. The cells were maintained at 37°C in a humidified atmosphere containing 5% CO₂. Before experiments, cells were cultured under serum-free conditions in M199 medium for 18 to 24 h. For hypoxia treatment, cells were cultured under hypoxic conditions (1% O₂, 5% CO₂ and 94% N₂) and harvested at different times. Anti-*NDRG2* (1:500 dilution) antibodies were purchased from BD Corporation (BD, NY, USA). Anti-HIF-1 α (1:200 dilution) and anti-p53 (1:1000 dilution) antibodies, and ECL reagents were from Santa Cruz Technology (Santa Cruz, CA, USA). Anti-VHL antibody (1:200 dilution) was from Neomarkers Corporation (Taipei, China).

Anti- β -actin antibody (1:5000 dilution) was from Sigma (Sigma, USA).

Gene infection

A multiplicity of infection (MOI) of 40 was determined experimentally for MCF-7 cells. Cells were seeded in 6-well plates at a density of 5×10^5 cells/well and incubated to reach approximately 80% confluence. After removing the medium, adenovirus expressing *NDRG2* (Ad-*NDRG2*) or the negative control gene LacZ (Ad-LacZ) was added in serum-free DMEM, incubated for 2 h, replaced with fresh DMEM supplemented with 10% FBS and incubated for 48 h.

Gene transfection

MCF-7 cells were seeded in 6-well plates at a density of 5×10^5 cells/well and incubated to reach approximately 80% confluence. The gene transfection assay was performed with the following constructs using Lipofectamine 2000 (Invitrogen, Carlsbad, Calif) according to the manufacturer's instructions: a small interfering RNA (siRNA) that targeted *NDRG2* (si*NDRG2*: forward, GCU-CUCUGGAAAUCUGAGUUGAUA; reverse, UUAAGAGC-AUAUCUCGCCAGGAUGU) and its scramble siRNA (scramble: forward, UUCUCCGAACGUGUCACGUTT; reverse, AC-GUGACACGUUCGGAGAATT; Biomics Inc., AgouraHills, Calif). Cells were exposed to siRNA in DMEM for 6 h, after

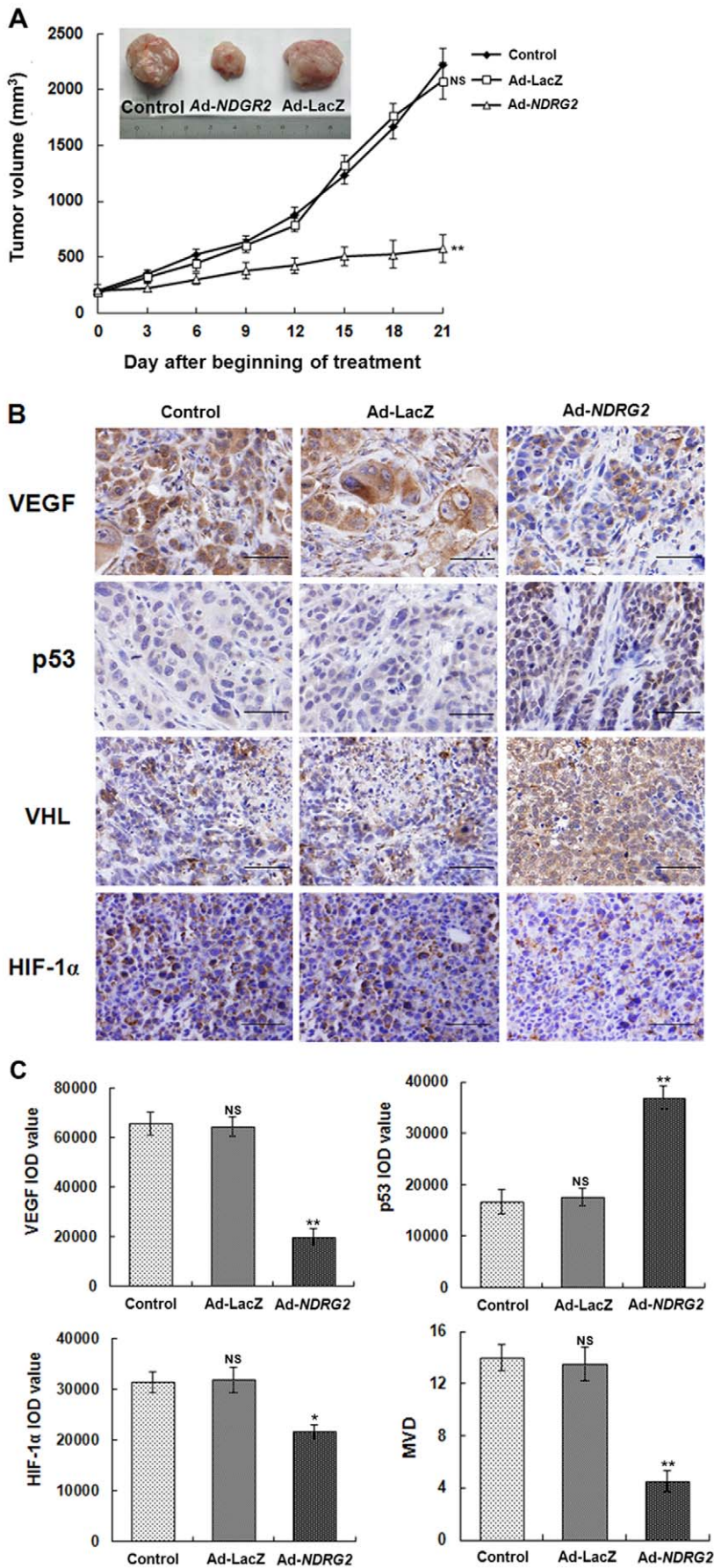


Figure 5. Effects of intratumoral injections of Ad-*NDRG2* on the growth and vascularization of MCF-7 cell xenografts in mice. These experiments were described in "Materials and Methods". (A) Tumor growth curve. The tumor growth was assessed every 3 days until Day 21 of treatment by measuring two perpendicular diameters and calculating the volume in mm³. Statistical analysis was performed using Day 21 values only, with one-way ANOVA and Student's *t*-test. ** indicates $P < 0.01$ when compared with the control. The typical photographs of tumors are shown. (B) Intratumoral vascularization was assessed by VEGF, p53, VHL, and HIF-1 α immunolabeling (400 \times magnification) on paraffin-embedded MCF-7 cell tumor sections. Representative images are shown. (C) Integrated optical density (IOD) values of VEGF, p53, VHL, HIF-1 α protein expression and MVD of the tumors were evaluated. ImagePro Plus software was utilized to analyze the IOD values of the positive areas of immunohistochemical staining, and the resulting histograms are shown. After areas containing dense vascularity, either within the tumor or during different pathological stages, were selected using a microscopic field with 100 \times power, all brown-stained vessels were counted under three fields with 200 \times power. The mean value of the vessels in the three fields was taken as the MVD count of a tumor. The histograms are shown. Statistical analysis was carried out using one-way ANOVA. The results are shown as the mean \pm SD from a total of six mice. * $P < 0.05$ or ** $P < 0.01$. doi:10.1371/journal.pone.0032368.g005

which the medium was replaced with DMEM containing 10% FBS and the cells were incubated for 48 h.

RT-PCR

RNA extracted from cells with Trizol reagent (Invitrogen, Life Technologies, US) was converted to cDNA using the RevertAidTM First Strand cDNA Synthesis Kit (Fermentas, CA). Total RNA (5 μ g) was then reverse transcribed into cDNA using an AMV reverse transcriptase (Promega, Madison, WI, USA) according to the manufacturer's instructions. The cDNA was subjected to PCR amplification using the following primers: *NDRG2*, 5'-ATGGCG-GAGCTGCAGGAGGTGC-3' (sense) and 5'-TGAGGAACG-AGGTCTGGGTGGG-3' (antisense); β -actin, 5'-GATCATT-GCTCCTCCTGAGC-3' (sense) and 5'-TGTGGACTTGGGA-GAGGACT-3' (antisense). The PCR mixture (25 μ l) containing a Taq polymerase from Promega was denatured at 94°C for 5 min, followed by 35 cycles of 94°C for 30 s, 60°C for 30 s and 72°C for 30 s, with a final extension at 72°C for 10 min. The PCR products were separated in 3% agarose gels by electrophoresis and visualized with ethidium bromide under a UV light.

Western blot

MCF-7 cells were homogenized in RIPA lysis buffer and insoluble material was removed by centrifugation at 4°C. From each sample, 80–100 μ g of total protein extract was resolved by 12% SDS-PAGE and transferred to nitrocellulose membranes (Amersham Biosciences, Piscataway, NJ). The membranes were blocked in 5% milk and probed with the antibodies overnight at 4°C. Membranes were washed and incubated with a horseradish peroxidase (HRP)-conjugated secondary antibody (Santa Cruz Biotech) for 1 h at 37°C. Chemiluminescent HRP substrate solution (Millipore, USA) was used to develop the images.

MTT assay

HUVECs were plated at a density of 4×10^4 cells/cm² in 24-well plates in complete medium and allowed to adhere overnight. The conditioned culture medium from MCF-7 cells was placed in the wells, and the whole plate was incubated in a hypoxic chamber. HUVEC proliferation was measured using a modified MTT (3-(4,5-dimethylthiazol-2-yl)-2,5-diphenyl tetrazolium bromide) assay. After the inserts were removed, 100 μ l MTT was added per well, and HUVECs were incubated for 4 h. The formazan crystals formed were dissolved in 750 μ l dimethyl sulfoxide after the medium was aspirated. The solution was transferred to a 96-well plate and the optical density value was recorded at 570 nm on a Microplate Reader (Model 680, Bio-Rad, USA). The results were expressed relative to the OD value of HUVEC monocultures on day 1 of the assay.

ELISA assay

To assess VEGF secretion in the supernatants of infected cells, the cells were incubated in serum-free medium under normoxia or

hypoxia. After 0–36 h, the media were collected, centrifuged to remove cellular debris, and stored at -70°C until assayed for VEGF. VEGF secreted in the culture medium was measured by ELISA according to the manufacturer's instructions. Data were expressed in pg VEGF/ 10^5 cells/ml.

Tube formation assay

Sterile 24-well plates were coated with 200 μ l Matrigel and incubated at 37°C for 1 h to form gels. After polymerization of the gels, 1.0×10^5 HUVECs were seeded into each well and incubated with 1.0 ml DMEM containing 1% FBS. Next, media from MCF-7 cells were placed in the wells under hypoxia for 6 h. Five different fields were chosen randomly in each well, and photographs were taken. The length of the tubes was measured using Image-Pro Plus software (Media Cybernetics, L.P., Silver Spring, MD, USA) and was expressed as total length (mm) per microscopic field for each well.

Invasion assay

The HUVECs migration assay was performed using Matrigel-coated, Costar Transwell inserts with an 8 μ m pore-size. Briefly, 5.0×10^4 HUVECs were seeded onto inserts and incubated with M199 medium containing 1% FBS. After a 1 h attachment, the inserts were transferred to 24-well plates containing media from Ad-LacZ-MCF-7 or Ad-*NDRG2*-MCF-7 cells. After incubation for 4 h under hypoxic condition, the inserts were fixed with 4% paraformaldehyde and stained with hematoxylin and eosin. The number of invaded cells was counted using phase contrast microscopy (400 \times). Five randomly chosen fields were counted per insert.

Xenograft study in nude mice

For inoculation into nude mice, MCF-7 cells were washed with PBS, digested with trypsin, and resuspended in serum-free DMEM medium. After centrifugation (800 rpm), cell pellets were resuspended in DMEM. The cell suspension (5×10^6 cells in a volume of 100 μ l PBS) was injected subcutaneously into the hind legs of 4-week-old female BALB/C athymic (nu/nu) mice (SLAC Laboratory Animal Company, Shanghai, China) [24]. When tumors reached a volume of 200 mm³, the mice were arbitrarily assigned to different groups ($n = 6$ each) to receive intratumoral injections of 10^9 PFU Ad-*NDRG2*, Ad-LacZ, or PBS. Intratumoral injections were repeated every 3 days for a total of 20 days. Tumors were measured (perpendicular diameters) every day and their volumes calculated. On day 20, the mice were sacrificed and their tumors removed for analysis. Tumor volumes were calculated based on caliper measurements of the length and width of the lesions using the following formula: $0.5 \times \text{length} \times \text{width}^2$. The growth curve was then derived from these data.

All the experimental procedures were conducted in accordance with the Detailed Rules for the Administration of Animal Experiments for Medical Research Purposes issued by the

Ministry of Health of China and received ethical approval by the Animal Experiment Administration Committee of the Fourth Military Medical University (Xi'an, P. R. China). All efforts were made to minimize the animals' suffering and to reduce the number of animals used.

Immunohistochemistry

Immunohistochemical staining was performed to assess the protein expression of VEGF, HIF-1 α , VHL, p53 and CD31, as described previously [25]. For immunohistochemistry, formalin-fixed tumor tissues were embedded in paraffin, and serial 4 μ m sections were obtained using a Leica microtome. For staining, tumor sections were dewaxed in toluene, rehydrated in an alcohol gradient, permeabilized in citrate buffer (pH 6.0), quenched with 3% H₂O₂ for 5 min to eliminate endogenous peroxidase activity, washed in PBS, incubated overnight with different antibodies and then with biotinylated goat anti-rat or anti-rabbit IgG antibody for 15 min. After washing, sections were incubated with streptavidin-

peroxidase, lightly counterstained with hematoxylin, and observed under a photomicroscope.

Statistical analysis

SPSS 13.0 software was used to perform statistical analyses. Data are presented as the mean \pm SD, and statistical comparisons between groups were made using one-way ANOVA followed by Student's *t*-test. *P* < 0.05 was considered statistically significant.

Author Contributions

Conceived and designed the experiments: JM. Performed the experiments: XY QW LW. Analyzed the data: YX SL LM LY. Contributed reagents/materials/analysis tools: QZ HR YC. Wrote the paper: JM. Critical revision of the manuscript for important intellectual content and study supervision: WL. Study concept and design, obtained funding, critical revision of the manuscript for important intellectual content and study supervision: JZ.

References

- Munoz-Najar UM, Neurath KM, Vumbaca F, Claffey KP (2006) Hypoxia stimulates breast carcinoma cell invasion through MT1-MMP and MMP-2 activation. *Oncogene* 25: 2379–2392.
- Yang XM, Wang YS, Zhang J, Li Y, Xu JF, et al. (2009) Role of PI3K/Akt and MEK/ERK in mediating hypoxia-induced expression of HIF-1 α and VEGF in laser-induced rat choroidal neovascularization. *Invest Ophthalmol Vis Sci* 50: 1873–1879.
- Dewhirst MW (2009) Relationships between cycling hypoxia, HIF-1, angiogenesis and oxidative stress. *Radiat Res* 172: 653–665.
- Wang YQ, Luk JM, Ikeda K, Man K, Chu AC, et al. (2004) Regulatory role of vHL/HIF-1 α in hypoxia-induced VEGF production in hepatic stellate cells. *Biochem Biophys Res Commun* 317: 358–362.
- Sikora S, Godzik A (2004) Combination of multiple alignment analysis and surface mapping paves a way for a detailed pathway reconstruction—the case of VHL (von Hippel-Lindau) protein and angiogenesis regulatory pathway. *Protein Sci* 13: 786–796.
- Chen D, Li M, Luo J, Gu W (2003) Direct interactions between HIF-1 α and Mdm2 modulate p53 function. *J Biol Chem* 278: 13595–13598.
- Pal S, Datta K, Mukhopadhyay D (2001) Central role of p53 on regulation of vascular permeability factor/vascular endothelial growth factor (VPF/VEGF) expression in mammary carcinoma. *Cancer Res* 61: 6952–6957.
- Deng Y, Yao L, Chau L, Ng SS, Peng Y, et al. (2003) N-Myc downstream-regulated gene 2 (NDRG2) inhibits glioblastoma cell proliferation. *Int J Cancer* 106: 342–347.
- Zhou RH, Kokame K, Tsukamoto Y, Yutani C, Kato H, et al. (2001) Characterization of the human NDRG gene family: a newly identified member, NDRG4, is specifically expressed in brain and heart. *Genomics* 73: 86–97.
- Yao L, Zhang J, Liu X (2008) NDRG2: a Myc-repressed gene involved in cancer and cell stress. *Acta Biochim Biophys Sin (Shanghai)* 40: 625–635.
- Zhang J, Li F, Liu X, Shen L, Liu J, et al. (2006) The repression of human differentiation-related gene NDRG2 expression by Myc via Miz-1-dependent interaction with the NDRG2 core promoter. *J Biol Chem* 281: 39159–39168.
- Gao L, Wu GJ, Liu XW, Zhang R, Yu L, et al. (2011) Suppression of invasion and metastasis of prostate cancer cells by overexpression of NDRG2 gene. *Cancer Lett* 310: 94–100.
- Lorentzen A, Lewinsky RH, Bornholdt J, Vogel LK, Mitchelmore C (2011) Expression profile of the N-myc Downstream Regulated Gene 2 (NDRG2) in human cancers with focus on breast cancer. *BMC Cancer* 11: 14.
- Liu N, Wang L, Liu X, Yang Q, Zhang J, et al. (2007) Promoter methylation, mutation, and genomic deletion are involved in the decreased NDRG2 expression levels in several cancer cell lines. *Biochem Biophys Res Commun* 358: 164–169.
- Shon SK, Kim A, Kim JY, Kim KI, Yang Y, et al. (2009) Bone morphogenetic protein-4 induced by NDRG2 expression inhibits MMP-9 activity in breast cancer cells. *Biochem Biophys Res Commun* 385: 198–203.
- Zheng J, Liu Q, Li Y, Yang J, Ma J, et al. (2010) NDRG2 expression regulates CD24 and metastatic potential of breast cancer cells. *Asian Pac J Cancer Prev* 11: 1817–1821.
- Choi SC, Yoon SR, Park YP, Song EY, Kim JW, et al. (2007) Expression of NDRG2 is related to tumor progression and survival of gastric cancer patients through Fas-mediated cell death. *Exp Mol Med* 39: 705–714.
- Wang L, Liu N, Yao L, Li F, Zhang J, et al. (2008) NDRG2 is a new HIF-1 target gene necessary for hypoxia-induced apoptosis in A549 cells. *Cell Physiol Biochem* 21: 239–250.
- Ravi R, Mookerjee B, Bhujwala ZM, Sutter CH, Artemov D, et al. (2000) Regulation of tumor angiogenesis by p53-induced degradation of hypoxia-inducible factor 1 α . *Genes Dev* 14: 34–44.
- Nor JE, Christensen J, Mooney DJ, Polverini PJ (1999) Vascular endothelial growth factor (VEGF)-mediated angiogenesis is associated with enhanced endothelial cell survival and induction of Bcl-2 expression. *Am J Pathol* 154: 375–384.
- Krieg M, Haas R, Brauch H, Acker T, Flamme I, et al. (2000) Up-regulation of hypoxia-inducible factors HIF-1 α and HIF-2 α under normoxic conditions in renal carcinoma cells by von Hippel-Lindau tumor suppressor gene loss of function. *Oncogene* 19: 5435–5443.
- Baek JH, Jang JE, Kang CM, Chung HY, Kim ND, et al. (2000) Hypoxia-induced VEGF enhances tumor survivability via suppression of serum deprivation-induced apoptosis. *Oncogene* 19: 4621–4631.
- Blagosklonny MV, An WG, Romanova LY, Trepel J, Fojo T, et al. (1998) p53 inhibits hypoxia-inducible factor-stimulated transcription. *J Biol Chem* 273: 11995–11998.
- Pille JY, Denoyelle C, Varet J, Bertrand JR, Soria J, et al. (2005) Anti-RhoA and anti-RhoC siRNAs inhibit the proliferation and invasiveness of MDA-MB-231 breast cancer cells in vitro and in vivo. *Mol Ther* 11: 267–274.
- Zheng J, Li Y, Yang J, Liu Q, Shi M, et al. (2011) NDRG2 inhibits hepatocellular carcinoma adhesion, migration and invasion by regulating CD24 expression. *BMC Cancer* 11: 251: 251–259.